IEEE Photonics Journal
An IEEE Photonics Society Publication

1-Gb/s Transmission Over a Phosphorescent White LED by Using Rate-Adaptive Discrete Multitone Modulation

Volume 4, Number 5, October 2012

A. M. Khalid
G. Cossu
R. Corsini
P. Choudhury
E. Ciaramella

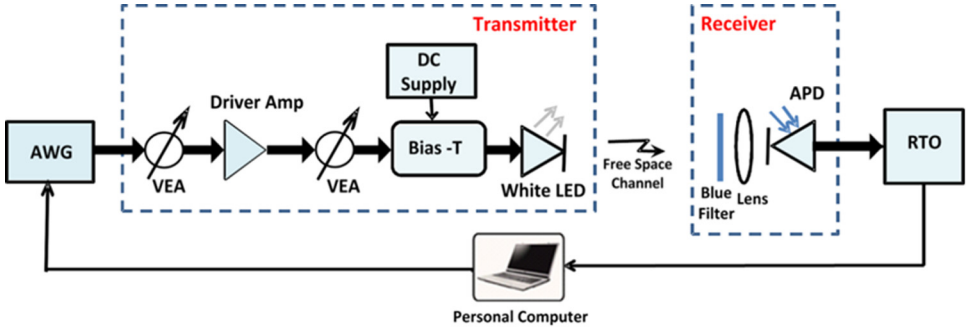

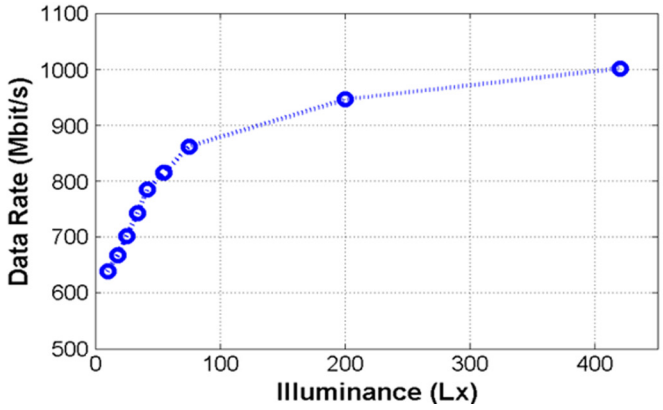

DOI: 10.1109/JPHOT.2012.2210397
1943-0655/$31.00 ©2012 IEEE

1-Gb/s Transmission Over a Phosphorescent White LED by Using Rate-Adaptive Discrete Multitone Modulation

A. M. Khalid, G. Cossu, R. Corsini, P. Choudhury, and E. Ciaramella

Scuola Superiore Sant'Anna—TeCIP, 56124 Pisa, Italy

DOI: 10.1109/JPHOT.2012.2210397
1943-0655/$31.00 ©2012 IEEE

Manuscript received June 29, 2012; accepted July 20, 2012. Date of publication July 26, 2012; date of current version August 8, 2012. Corresponding author: A. M. Khalid (e-mail: a.khalid@sssup.it).

Abstract: Light-emitting diodes (LEDs), which will be increasingly used in lighting technology, will also allow for distribution of broadband optical wireless signals. Visible-light communication (VLC) using white LEDs offers several advantages over the RF-based wireless systems, i.e., license-free spectrum, low power consumption, and higher privacy. Mostly, optical wireless can provide much higher data rates. In this paper, we demonstrate a VLC system based on a white LED for indoor broadband wireless access. After investigating the nonlinear effects of the LED and the power amplifier, a data rate of 1 Gb/s has been achieved at the standard illuminance level, by using an optimized discrete multitone modulation technique and adaptive bit- and power-loading algorithms. The bit-error ratio of the received data was $1.5 \cdot 10^{-3}$, which is within the limit of common forward error correction (FEC) coding. These results twice the highest capacity that had been previously obtained.

Index Terms: Free-space optics, visible-light communication (VLC), discrete multitone, phosphorescent white LED.

1. Introduction

In future illumination systems, white light-emitting diodes (LEDs) will replace the conventional fluorescent and incandescent lamps [1]. LEDs offer several advantages over traditional light sources, such as low power consumption, low cost, high luminance efficiency, ease in color rendering, and long lifetime. Furthermore, LEDs can be directly modulated and used as optical transmitters to realize wireless data transmission links. This emerging communication technology, which utilizes white LEDs for both illumination and data transmission, is known as visible-light communication (VLC). VLC has recently took much attention for future indoor wireless communication, since VLC systems also provide high security and do not suffer from electromagnetic interferences (EMIs) [2]. Moreover, LEDs can reach much higher data rates than RF signals.

Typically, white illumination is achieved by blue-emitting LEDs coated with a phosphor layer. The bandwidth of the commercial phosphor-based LEDs is thus limited to a few megahertz (typically 2–3 MHz [3]), because of the slow response of the phosphors. In order to overcome this limitation, a blue filter at the receiver can be used to suppress the slow phosphorescent components; this increases the bandwidth up to 20 MHz [4].

A data rate of more than 100 Mb/s was demonstrated using OOK modulation with PIN or APD receivers and blue filter [5]. In order to further increase the data rate, spectrally efficient modulation techniques such as orthogonal frequency-division multiplexing (OFDM) or discrete multitone (DMT)

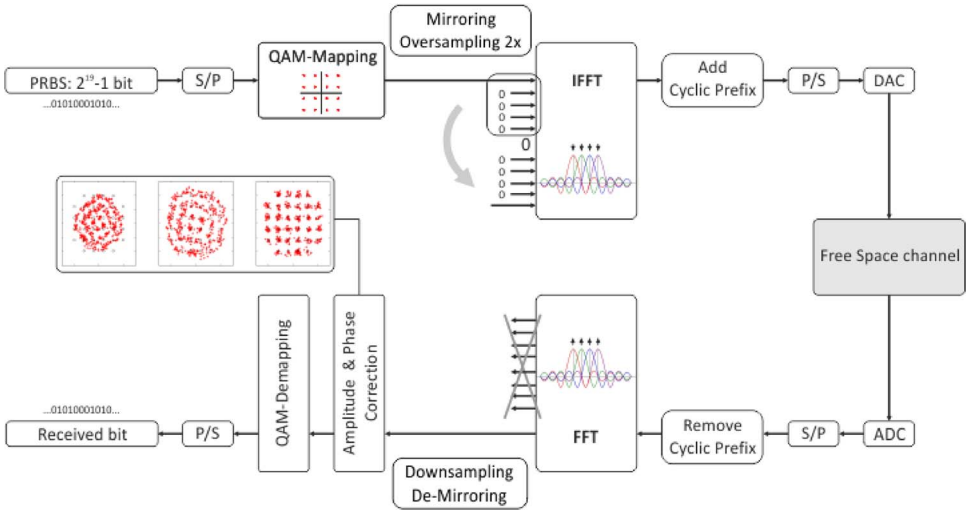

Fig. 1. Block diagram of DMT implementation.

can be used [6], [7]. Recently, a 513-Mb/s transmission rate has been achieved using a phosphor-based white LED modulated by a DMT signal [8].

In this paper, we report 1-Gb/s VLC systems using a white LED and the DMT signal. First, we analyzed the impact of the nonlinear characteristic of the electrical amplifier and the LED on the bit-error-ratio (BER) performance. The effect of the number of subcarriers was then evaluated in order to maximize the overall capacity. From this analysis, we were able to experimentally demonstrate a VLC system having a 1-Gb/s transmission rate, which successfully employed an optimized DMT signal at the transmitter and an avalanche photodiode (APD) as a receiver.

The paper is organized as follows. In Section II, the implementation of the DMT signal and the experimental setup are reported. In Section III, we present and discuss the experimental results; finally, we give our conclusions in Section IV.

2. Experimental Details

2.1. DMT Implementation

While OFDM is known for its mass application in wireless fidelity (Wi-Fi) or wireless local area networks (WLANs) and terrestrial digital video broadcasting (DVB-T), DMT is commonly used in copper-based digital subscriber lines (DSLs) for high-speed Internet access via asymmetric DSL (ADSL) [9].

The key aspect of the DMT modulation scheme is to decompose a single-carrier signal into flat multiple subcarriers. The subcarriers have the minimum frequency separation required to maintain orthogonality of their corresponding time-domain waveforms, and the signal spectra correspond to the overlap in frequency of different subcarriers. If the knowledge of the channel response is available at the transmitter, the DMT signal can be adapted to match this channel. In practice, this is achieved by means of adaptive bit-loading techniques, optimizing the different sized signal constellations that are transmitted on the various subcarriers. Similarly, the distribution of the signal power over the subcarriers can be finely adapted to have similar BER performance, which leads to an efficient use of the channel capacity.

In Fig. 1, the principle of DMT is shown. A high-speed binary sequence is divided into N parallel binary streams, at lower speed. For each stream, the binary data are mapped into complex values, each corresponding to a symbol of a QAM constellation. The IFFT is used in the DMT transmitter to efficiently modulate the complex values in N different subcarrier frequencies that, as a result, are mutually orthogonal. To get a real signal, $2N$ information symbols are chosen to satisfy the Hermitian symmetry property (mirroring). After mirroring, zero padding is applied to introduce two-times

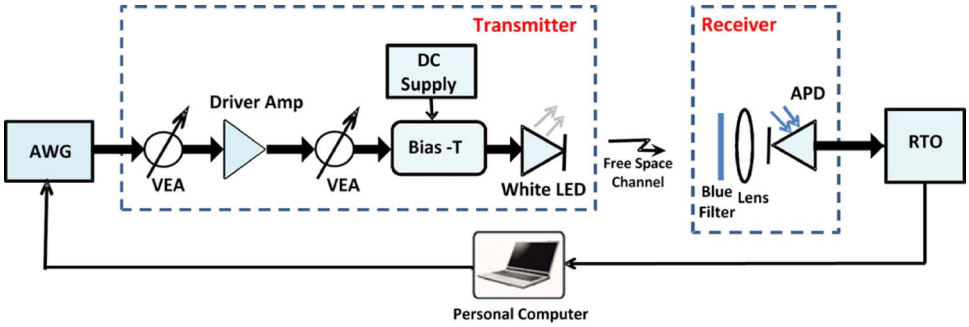

Fig. 2. Experimental setup of the VLC system. AWG: arbitrary waveform generator; VEA: variable electrical attenuator; RTO: real-time oscilloscope.

oversampling, leading to $4N$ subcarriers. The result of the $4N$-point IFFT is indeed a real-valued time signal referred to as DMT frame. To mitigate the effects of intersymbol interference (ISI) caused by channel time spread, each block of $4N$ IFFT points is typically preceded by a cyclic prefix (CP) consisting of N_{cp} samples. As a result, the effects of the ISI can be reduced. This $(4N + N_{cp})$-point sequence corresponds to the discrete-time samples of the multicarrier DMT time signal, which results from parallel-to-serial conversion of the IFFT output. The time-domain signal is fed to a digital-to-analog converter (DAC).

At the receiver, an FFT block is used to process the received signal after parallelization and removal of the CP. Ideally, the FFT output will be the original symbols that were sent to the IFFT at the transmitter. Normally, additional channel impairments must be estimated and properly dealt with. A training sequence was used for estimating the channel frequency response. This estimation allows to apply the zero-forcing equalization to the signal. After correction, the complex values are demapped, and the bit stream was obtained by a parallel-to-serial process. Finally, BER value was computed comparing the original sequence with the recovered bits.

2.2. Experimental Setup

The experimental setup is shown in Fig. 2. The optical source was a phosphor-based white LED generating a luminous flux of about 13 lm at 80-mA bias current with 120° Lambertian emission. The DMT waveform, consisting of 512 subcarriers in a bandwidth of 180 MHz, was uploaded into the arbitrary waveform generator (AWG, Tektronix 7102). The first carrier, corresponding to dc, was not modulated. The signal from the AWG was first amplified by a power amplifier (PA) (25-dB gain, and 29-dBm minimum output power at 1-dB compression; 130-MHz 3-dB bandwidth) to obtain an appropriate modulation index of the LED light. The electrical DMT signal was then superimposed on the LED dc bias current (80 mA) via a bias-T. The receiver module was in front of the LED and aligned to ensure the direct line-of-sight (LOS) between the Tx and Rx. The analog receiver was an APD module consisting of an APD (0.42-A/W responsivity at 620 nm; 0.8-mm^2 active area) and an integrated transimpedance amplifier (TIA, 100-MHz 3-dB bandwidth). A dichroic optical bandpass filter (Semrock, 97% transmissivity at 452 nm, with 45-nm FWHM bandwidth) was placed in front of the APD to reject the slow phosphorescent components, and a bi-convex glass lens (25.4-mm focal length, 25.4-mm diameter) was used to focus the light onto the APD active area. The output signal from the APD module was then sampled and stored by means of a real-time oscilloscope (Lecroy, 1 GSa/s) for offline demodulation.

3. Experimental Results and Discussion

3.1. Evaluation of DMT and Communication Link Parameters

The DMT modulation format makes the system very sensible to nonlinear distortions, because of the large dynamic range of the transmitted signal. In RF systems, the main source of nonlinearity is

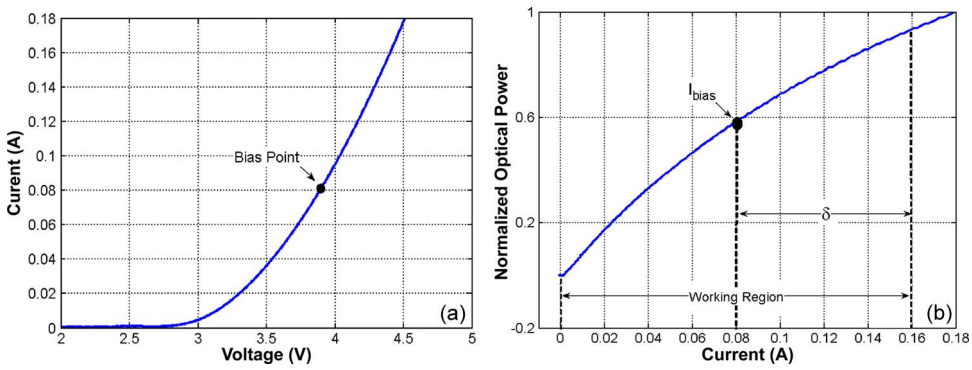

Fig. 3. (a) Current versus voltage characteristics of LED. (b) Normalized transfer function of the white LED.

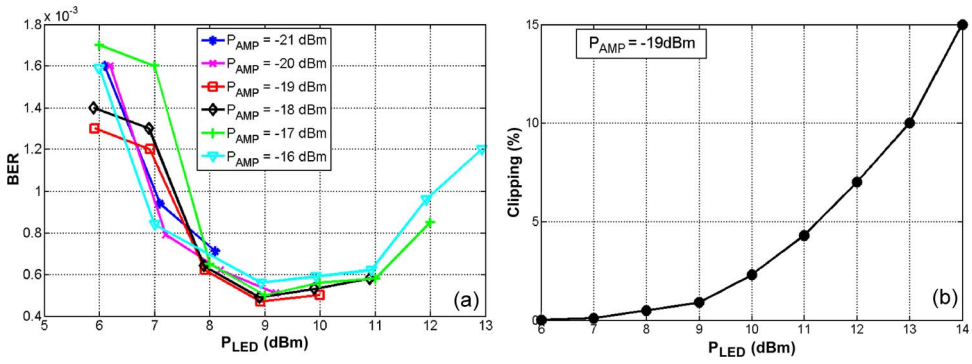

Fig. 4. (a) BER versus input power to LED P_{LED} at 900 Mb/s and at 420 lx. (b) Clipping percentage versus P_{LED}.

the PA [10]. If the PA operates near the saturation point, undesirable nonlinear effects introduce amplitude and phase distortions, which, in turn, can cause adjacent carrier interference and power losses, hence reducing the overall system performance. On the other hand, an excessive back-off power leads to an under-modulation of the signal, resulting also in this case in degradation of the system performance.

In optical wireless communication systems, the LED shows significant nonlinearity [11], [12] due to the exponential behavior of current–voltage characteristics and of the nonlinear characteristics of the output power as a function of the input current. In Fig. 3(a), the measured current–voltage characteristics of the white LED used in the experiment is reported. The LED has a threshold value, usually indicated as turn-on voltage (TOV), of about 2.4 V. Above TOV, further increasing the voltage allows the current to flow and the output optical power increases nonlinearly as a function of the current, as we show in Fig. 3(b).

The LED should be operated within the allowed dc current limit in order to avoid reduction in electrooptical efficiency due to the temperature instability. From the datasheet, the maximum allowed dc current is 100 mA. In our experiment, we fixed our bias current to 80 mA.

The overall distortion levels can be controlled by changing the input power of PA and LED. The severities of nonlinear effects in terms of the BER degradation were measured at a fixed data rate (i.e., 900 Mb/s) and at 420 lx. In Fig. 4(a), we present the BER as a function of the input power to the LED (P_{LED}) for different input power to the amplifier (P_{AMP}). The input power P_{AMP} was varied between -16 dBm up to -21 dBm with 1-dB step. For each P_{AMP}, the P_{LED} was varied by 1-dB step over different ranges due to maximum available power. The lowest BER values were observed for P_{LED} in the range between $+8$ dBm to $+11$ dBm. In this range, the BER variation was less than 0.2 decades.

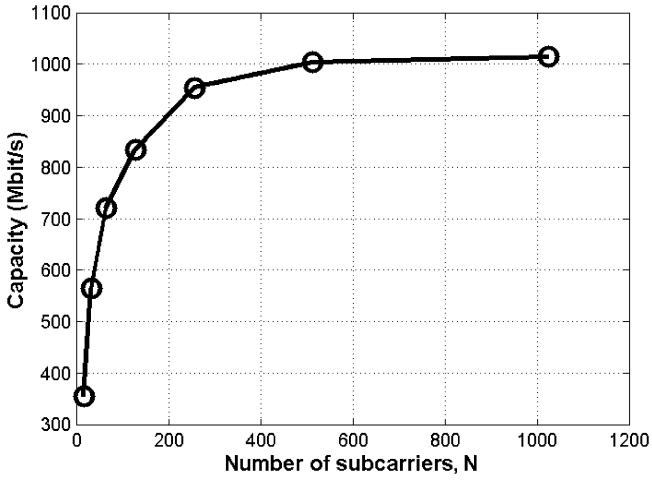

Fig. 5. Experimental capacity for the frequency-dependent VLC link.

For power levels below $+8$ dBm, low modulation depth was obtained; on the other hand, for power levels exceeding $+11$ dBm, BER values increase because of the distortions introduced by the clipping. In Fig. 4(b), we report the calculated clipping percentage of the DMT waveform as a function of P_{LED}. Increasing P_{LED}, the lower part of the DMT signal goes below TOV, producing a deformed modulated waveform. In our measurement, we thus fixed the LED power at $+9$ dBm (clipping $< 1\%$). At this power level, the current variation corresponding to the ± 3 sigma of the DMT signal distribution was $\delta = 80$ mA, inducing a current swing between $I_{bias} - \delta$ and $I_{bias} + \delta$. The resulting modulation index m is given by [11]

$$m = \frac{\delta}{I_{bias}} = 1 \tag{1}$$

From the experimental data, we conclude that it is better to operate the LED with high modulation index accepting some distortion rather than driving the LED in linear regime with low m. The optimum input power of the driver amplifier was $P_{AMP} = -19$ dBm at $P_{LED} = +9$ dBm. Increasing P_{AMP}, the amplifier started to generate nonlinear components that distort the signal and produce a deterioration of the BER. The values of -19 dBm and $+9$ dBm were then chosen as working point for the PA and for the LED, respectively. The driver amplifier was operating well below the saturation power level, with 20-dB output power back-off.

The number of DMT subcarriers N was also optimized in order to maximize the performance of the VLC link. Using a DMT signal of bandwidth B (in our case, we set it to 180 MHz), the total bit rate b_{tot} is obtained by

$$b_{tot} = \frac{B}{N} \sum_{i=2}^{N} b_i \tag{2}$$

where b_i indicates the number of bits per symbol per carrier. For a frequency-selective channel, a large number of subcarriers can be effectively combined with the use of adaptive bit/power-loading, so that the modulation format and power per channel is finely optimized to the available signal-to-noise ratio (SNR) at each particular frequency. Therefore, the finer is the allocations into N subchannels, the better will be the optimization of the DMT. In Fig. 5, we report the data rate as a function of the number of subcarriers N. The curve shows the measured capacity for the frequency-dependent VLC link by employing rate-adaptive bit-loading for different $N = 2^n$ subcarrier, where $n = 4, 5, \ldots, 10$. The performance improvements obtained with a higher number of subcarrier are

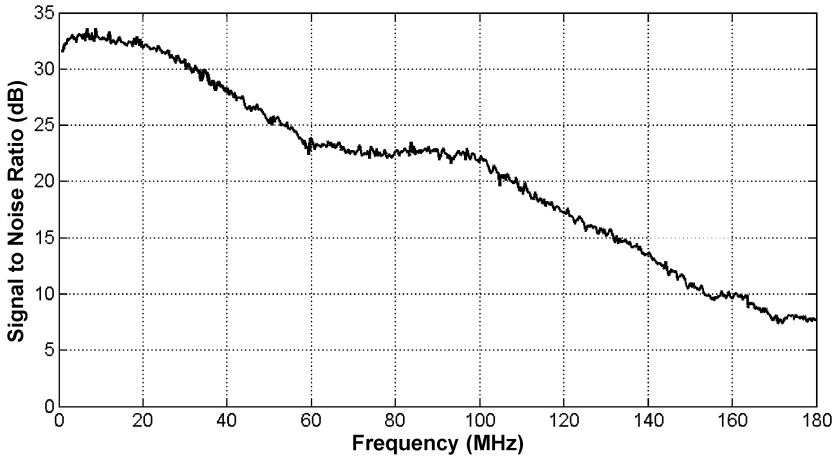

Fig. 6. Estimated SNR of the VLC channel as a function of the frequency.

due to the better estimation of the amplitude and phase response performed by the used zero-forcing equalizer in case of high frequency-selective channel. In terms of capacity achievable, we observed that the data rate increases significantly from 354 Mb/s up to 1 Gb/s when moving from 16 to 512 subcarriers. The BER of the measured capacity was always maintained less than $2 \cdot 10^{-3}$, which is the limit of the common forward error correction (FEC) algorithm [13]. For $N > 512$, the performance saturated and data rate did not increase significantly. On the other hand, increasing the number of subcarriers, the digital signal processing complexity increases, providing only 1% of capacity improvement. Therefore, 512 subcarriers are an optimum compromise between the data rate and complexity.

The gross data rate includes the CP (4%), the training sequence (2%) and FEC overhead of 7% should also be considered for the total overhead of 13%.

3.2. Transmission Experiment

The primary objective of the VLC systems is to provide high-speed wireless connectivity without affecting the general illumination of the indoor environment [14]. So, in our experiment, we considered the brightness level (illuminance level) in front of the photodiode as the most pertinent design parameter. Brightness levels were measured by a lux-meter placed exactly in front of the receiver unit. The measurements were performed changing the illuminance level at the receiver by adjusting the distance between the transmitter and receiver module.

We used only one white LED in this experiment, so varying the distance between the transmitter and the receiver from 10 cm to 50 cm, an illuminance level between 420 lx (at 10 cm) and 10 lx (at 50 cm) was observed. These brightness values were below the level of standard illuminance in the working environments as recommended in European Standards [15], which is 500 lx. In a real situation, a VLC link of several meters can be achieved by using light lamps consisting of several white LEDs, while keeping the standard illumination level.

As a first step, the channel frequency response was estimated (at 420 lx) using a DMT signal where all the subcarriers were modulated by a BPSK having equal power (DMT-BPSK). The SNR was estimated by the error vector magnitude (EVM) of the received constellations using the method presented in [16]. In Fig. 6, we report of the SNR versus frequency. During this step, we also take into account the sampling frequency offset [17]. This condition occurs when either analog-to-digital converter (ADC) or DAC samples take place too fast or too slowly. A sampler frequency offset is then introduced, which corresponds to a time shift that increases with the number of acquired samples. From the Fourier transform theory, we have

$$F(f(t \pm k\tau)) = \hat{f}(\omega)\exp(\pm ik\omega\tau) \tag{3}$$

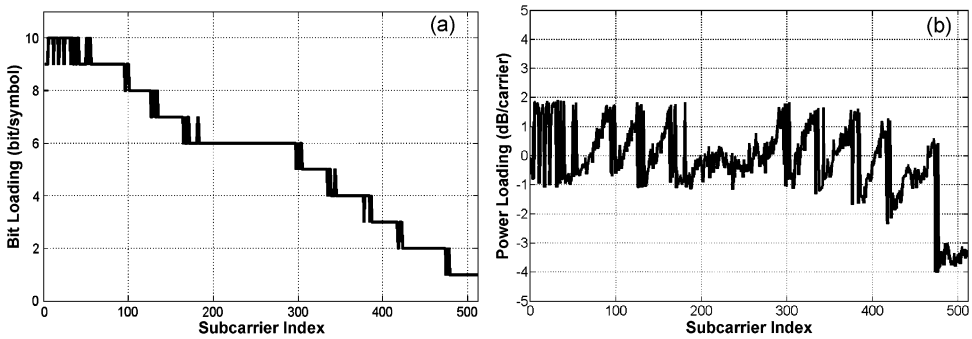

Fig. 7. Bit–power-loading distributions under the condition of BER $< 2 \cdot 10^{-3}$ at 420 lx. a) Optimal bit-loading distribution. b) Optimal power-loading distribution.

where F represents the Fourier transform, $f(t)$ is the acquired waveform, $\hat{f}(\omega) = F(f(t))$, k denotes the number of samples acquired, τ represents the time shift produced by the sampler frequency offset after a single sample, and ω is the frequency: When applied to a DMT signal, this gives that the detected symbol phase is affected by a spurious delay, which scales linearly with the frequency ω of the individual subcarriers.

The resulting SNR depends on how the receiver tracks this phase variation. After synchronization and zero-forcing equalization of the received DMT signal, the starting phase offset is zero. If no further phase correction is implemented, the constellation continuously rotates in time, increasing the EVM. We exploited the same DMT-BPSK signal used for SNR evaluation in order to estimate the variation of the phase in time and in frequency. Once this variation is known, the detected DMT signal can be corrected, effectively reducing the phase noise.

The algorithm adapted the signal to the channel by efficiently exploiting the available bandwidth and increasing the throughput to 1 Gb/s (the bits/symbol was increased when the SNR value was high and vice versa). A maximum of 1024 QAM (10 bits/symbol) was assigned to the subcarriers having an SNR of about 33 dB, whereas the BPSK (1 bit/symbol) format was chosen for the subcarriers having an SNR $<$ 9.2 dB. The distributions of bit- and power-loading [18] for the different subcarriers at 420 lx are reported in Fig. 7(a) and (b), respectively. The software left unmodulated any subcarriers with SNR $<$ 6.2 dB, which is the theoretical limit value for BPSK modulation (minimum bit-loading).

Fig. 7(b) presents the power distribution among the subcarriers that exhibit saw-tooth behavior. This means that in order to maintain the same QAM-level within a set of adjacent subcarriers at the same BER, the power allocated in that group increases with frequency following the inverse of the SNR curve.

In Fig. 8, we present the gross transmission capacity as a function of the illuminance at the receiver. The maximum gross data rate of 1 Gb/s was achieved at 420 lx (10 cm) with a total BER of $1.5 \cdot 10^{-3}$. The overall BER value was experimentally measured after offline demodulation of all the DMT frames composed of approximately 7 million bits. It can be noted that, at the illuminance level of only 10 lx (50 cm), we achieved 640 Mb/s. This allows reducing the LED intensity when required, while maintaining the high-speed connectivity. The saturation trend observed in Fig. 8 is mostly due to a focusing problem: at distances closer than 15 cm, the lens forms an image of the source larger than the APD active area; thus, the coupling efficiency is reduced. In a practical indoor VLC wireless links, the typical distances between the source and the transmitter should be 2–3 m, and the focusing problem described above would not be present and the link data rate could improve.

We expect that improvements can be obtained by optimizing the bandwidth of the driver amplifier and of the Rx (180 MHz). Additionally, further enhancement in the capacity could be achieved by increasing the efficiency of the amplifiers, operating them close to saturation and compensating the nonlinearities of both the amplifier and the LED [19], [20].

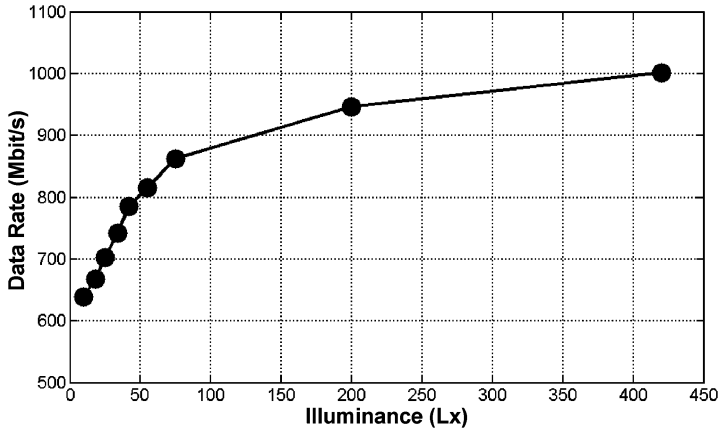

Fig. 8. Total measured capacity versus illuminance level at the receiver.

4. Conclusion

In this paper, we reported a 1-Gb/s LOS VLC link based on a commercial phosphorescent white LED and a common APD receiver. We evaluated the nonlinear effects generated by the driver amplifier and LED in terms of BER. The optimum working points in terms of amplifier input power, LED input power, and number of subcarriers of the DMT signal were obtained after a detailed experimental characterization. At these optimized conditions, a gross data rate of 1 Gb/s was achieved by using adaptive DMT modulation with a BER of $1.5 \cdot 10^{-3}$ (below the FEC limit). The bit- and power-loading techniques were effectively applied in order to efficiently exploit the limited available bandwidth of LED. It is shown that even at a very low illuminance level of 10 lx, a high-speed VLC link of 640 Mb/s can be obtained.

References

[1] J. K. Kim and E. F. Schubert, "Transcending the replacement paradigm of solid-state lighting," *Opt. Exp.*, vol. 16, no. 26, pp. 21 835–21 842, Dec. 2008.
[2] M. Z. Afgani, H. Haas, H. Elgala, and D. Knipp, "Visible light communication using OFDM," in *Proc. 2nd Int. Conf. TRIDENTCOM*, 2006, p. 134, 6 pp.
[3] T. Komine and M. Nakagawa, "Fundamental analysis for visible-light communication system using LED lightings," *IEEE Trans. Consum. Electron.*, vol. 50, no. 1, pp. 100–107, Feb. 2004.
[4] J. Grubor, K.-D. Langer, S. C. J. Lee, T. Koonen, and J. W. Walewski, "Wireless high-speed data transmission with phosphorescent white-light LEDs," in *Proc. 33rd Eur. Conf. Exhib. Opt. Commun.*, Sep. 16–20, 2007, pp. 1–2.
[5] J. Vucic, C. Kottke, S. Nerreter, K. Habel, A. Buttner, K.-D. Langer, and J. W. Walewski, "230 Mbit/s via a wireless visible-light link based on OOK modulation of phosphorescent white LEDs," in *Proc. Conf. OFC/NFOEC*, Mar. 21–25, 2010, pp. 1–3.
[6] A. M. Khalid, G. Cossu, R. Corsini, M. Presi, and E. Ciaramella, "Hybrid radio over fiber and visible light (RoF-VLC) communication system," in *Proc. 37th Eur. ECOC*, Sep. 18–22, 2011, pp. 1–3.
[7] H. Elgala, R. Mesleh, H. Haas, and B. Pricope, "OFDM visible light wireless communication based on white LEDs," in *Proc. IEEE 65th VTC-Spring*, Apr. 22–25, 2007, pp. 2185–2189.
[8] J. Vucic, C. Kottke, S. Nerreter, K. Langer, and J. W. Walewski, "513 Mbit/s visible light communications link based on DMT-modulation of a white LED," *J. Lightw. Technol.*, vol. 28, no. 24, pp. 3512–3518, Dec. 15, 2010.
[9] Asymmetric Digital Subscriber Line (ADSL), ITU Standard G.992.1, 1999.
[10] C.-P. Liang, J.-H. Jong, W. E. Stark, and J. R. East, "Nonlinear amplifier effects in communications systems," *IEEE Trans. Microw. Theory Tech.*, vol. 47, no. 8, pp. 1461–1466, Aug. 1999.
[11] B. Inan, S. C. J. Lee, S. Randel, I. Neokosmidis, A. M. J. Koonen, and J. W. Walewski, "Impact of LED nonlinearity on discrete multitone modulation," *IEEE/OSA J. Opt. Commun. Netw.*, vol. 1, no. 5, pp. 439–451, Oct. 2009.
[12] H. Elgala, R. Mesleh, and H. Haas, "A study of LED nonlinearity effects on optical wireless transmission using OFDM," in *Proc. IFIP Int. Conf. WOCN*, Apr. 28–30, 2009, pp. 1–5.
[13] Interfaces for the Optical Transport Network (OTN), ITU-T Recommendation, G.709/Y.1331.
[14] J. Grubor, S. Randel, K.-D. Langer, and J. W. Walewski, "Broadband information broadcasting using LED-based interior lighting," *J. Lightw. Technol.*, vol. 26, no. 24, pp. 3883–3892, Dec. 15, 2008.

[15] *Lighting of Indoor Work Places*, Eur. Standard EN 12464-1, 2003.
[16] R. A. Shafik, S. Rahman, and A. H. M. Razibul Islam, "On the extended relationships among EVM, BER and SNR as performance metrics," in *Proc. ICECE*, Dec. 19–21, 2006, pp. 408–411.
[17] J. Armstrong, "OFDM for optical communications," *J. Lightw. Technol.*, vol. 27, no. 3, pp. 189–204, Feb. 1, 2009.
[18] D. Hughes-Hartogs, "Ensemble modem structure for imperfect transmission media," U.S. Patent 4 833 796, May 1989.
[19] A. Katz, "Linearization: Reducing distortion in power amplifiers," *IEEE Microw. Mag.*, vol. 2, no. 4, pp. 37–49, Dec. 2001.
[20] H. Elgala, R. Mesleh, and H. Haas, "Predistortion in Optical Wireless Transmission Using OFDM," in *Proc. 9th Int. Conf. HIS*, Aug. 12–14, 2009, vol. 2, pp. 184–189.